

An Approach to Working Up Cases of Embolic Stroke of Undetermined Source

Sookyung Ryoo, MD; Jong-Won Chung, MD; Mi Ji Lee, MD; Suk Jae Kim, MD, PhD; Jin Soo Lee, MD, PhD; Gyeong-Moon Kim, MD, PhD; Chin-Sang Chung, MD, PhD; Kwang Ho Lee, MD, PhD; Ji Man Hong, MD, PhD; Oh Young Bang, MD, PhD

Background—From a therapeutic viewpoint, it is important to differentiate the underlying causes of embolism in patients with cryptogenic stroke, such as aortic arch atheroma, patent foramen ovale, and paroxysmal atrial fibrillation. We investigated the clinical and radiological characteristics of these 3 common causes of cryptogenic embolism to develop models for decision making in etiologic workups.

Methods and Results—A total of 321 consecutive patients with acute infarcts from cryptogenic embolism were included. Patients were divided into 3 groups—aortic arch atheroma (n=40), patent foramen ovale (n=153), and paroxysmal atrial fibrillation (n=128)—based on extensive cardiologic workups. We used a multinomial logistic regression analysis to detect the clinical and diffusion-weighted imaging factors associated with the probability of aortic arch atheroma, patent foramen ovale, and paroxysmal atrial fibrillation. Clinical and radiological features differed among the groups. The patent foramen ovale group had a healthy vascular risk factor profile and showed posterior circulation involvement compared with other groups ($P<0.01$). In contrast, paroxysmal atrial fibrillation-related strokes had higher initial National Institutes of Health Stroke Scale (NIHSS) scores and larger lesions than the other groups ($P<0.001$). The aortic arch atheroma group had clinical features similar to those of the paroxysmal atrial fibrillation group but showed small lesions scattered in multiple vascular territories ($P<0.001$). Multivariate regression analysis revealed that age, initial NIHSS score, lesion size (≥ 20 mm), multiple (≥ 3) lesions, and involvement of posterior circulation or multiple vascular territories differentiated the 3 groups (pseudo, $R^2=0.656$). The prediction ability of this model was validated in the external validation cohort (n=117, area under the curve 0.78).

Conclusions—Our data indicate that patients with cryptogenic embolic stroke show distinct clinical and radiological features depending on the underlying causes. (*J Am Heart Assoc.* 2016;5:e002975 doi:10.1161/JAHA.115.002975)

Key Words: cerebral infarction • diagnosis • embolic stroke of undetermined etiology • embolism

Embolic stroke of undetermined source is a common stroke subtype that accounts for 23% to 40% of all strokes.^{1–3} Appropriate investigation of the underlying causes is important for reducing the proportion of patients diagnosed with embolic stroke of undetermined source, thereby facili-

tating therapy implementation to target the underlying cause of the index stroke. Anticoagulation therapy, for example, is appropriate for patients with paroxysmal atrial fibrillation (PAF) because recurrent strokes are often of the same subtype as the preceding index stroke.

A gold standard for individualized workup after a stroke is lacking, although some procedures include brain imaging to differentiate ischemic from hemorrhagic stroke, vascular study, blood tests (eg, glucose and lipid profiles), and ECG. Workup costs may differ greatly, even among regions with the same socioeconomic status.⁴ As the number of tests has increased with advances in diagnostic techniques, workup costs have also continuously risen. Costs could be reduced by avoiding expensive but ineffective tests.⁴ Targeted selection and judicious use of the appropriate tests for embolic stroke of undetermined source in stroke workups are crucial. Although extensive pathogenic workups generally decrease the number of undetermined cases, they may also paradoxically increase the prevalence of embolic stroke of undetermined source. Although transesophageal echocardiography

From the Department of Neurology, Samsung Medical Center, Sungkyunkwan University School of Medicine, Seoul, South Korea (S.R., J.-W.C., M.J.L., S.J.K., G.-M.K., C.-S.C., K.H.L., O.Y.B.); Department of Neurology, Ajou University Hospital, Ajou University School of Medicine, Suwon, South Korea (J.S.L., J.M.H.).

An accompanying Data S1 is available at <http://jaha.ahajournals.org/content/5/3/e002975/suppl/DC1>

Correspondence to: Oh Young Bang, MD, PhD, Department of Neurology, Samsung Medical Center, Sungkyunkwan University, 81, Irwon-Ro, Gangnam-gu, Seoul 135–710, South Korea. E-mail: ohyoung.bang@samsung.com
Received November 27, 2015; accepted February 24, 2016.

© 2016 The Authors. Published on behalf of the American Heart Association, Inc., by Wiley Blackwell. This is an open access article under the terms of the Creative Commons Attribution-NonCommercial License, which permits use, distribution and reproduction in any medium, provided the original work is properly cited and is not used for commercial purposes.

(TEE), for example, may reveal high-risk sources with indication for oral anticoagulation,⁵ imprudent use may inadvertently lead to a rise in cases with ≥ 2 determined causes. Patent foramen ovale (PFO) is prevalent in both the general population and among stroke patients, whereas aortic arch atheroma (AAA) is commonly observed in elderly patients with multiple vascular risk factors. The probability of having PFO or AAA as a cause of, or coincident with, stroke should be weighted in patients with embolic stroke of undetermined source along with PFO or AAA.⁶

Diagnostic investigations of suspected cases of embolic stroke of undetermined source, particularly with advanced diagnostic techniques, should be guided and chosen in accordance with patient characteristics at the time of clinical presentation. The cost-effectiveness of advanced diagnostic technologies will greatly depend on the appropriate selection of patients for the various diagnostic tests. Kent and colleagues recently reported on the clinical and imaging characteristics of PFO that are likely to be stroke related or incidental, using the Risk of Paradoxical Embolism (RoPE) score⁷; however, no studies have evaluated the probability of PAF, PFO, and AAA in patients with embolic stroke of undetermined source. In the current study, we investigated the clinical and radiological characteristics of these 3 common causes of embolic stroke of undetermined source to develop a prediction model to help with decision making during etiologic workups.

Methods

Patients and Workups

Two separate data sets from different hospitals were used to develop and validate a prediction model. For model development, we prospectively recruited patients with acute ischemic stroke who were admitted to the Samsung Medical Center (a tertiary university hospital in Seoul, Republic of Korea) from September 2008 through September 2014. We used a prospective cohort from the Ajou University Hospital (a tertiary university hospital in Suwon, Republic of Korea) during the same period to test the model's performance. From patients who experienced focal or lateralizing neurological symptoms within 7 days from onset and had relevant lesions on diffusion-weighted imaging (DWI), we enrolled patients with stroke due to an undetermined cause at the time of admission. All patients underwent ECG and brain magnetic resonance imaging and magnetic resonance angiography in the emergency room. We excluded patients if they had a determined cause of stroke before admission, based on the Stop Stroke Study Trial of Org 10172 in Acute Stroke Treatment (SSS-TOAST; eg, significant stenosis of relevant arteries on magnetic resonance angiography or atrial fibrilla-

tion [usually permanent] on the first ECG). Local institutional review boards approved this study. All participants or patient guardians provided informed consent.

The following data were systematically collected: demographic information; medical history of vascular risk factors such as hypertension, diabetes mellitus, dyslipidemia, and smoking history; and initial National Institutes of Health Stroke Scale (NIHSS) scores. In addition, we performed extensive workups, including repetitive ECGs, transthoracic echocardiography or TEE, echo bubble tests or transcranial right-to-left shunt tests, multidetector row computed tomography (MDCT), and cardiac telemetry (≥ 72 hours). The transcranial right-to-left shunt test is based on the intracranial detection of intravenously injected microemboli. The size and functional relevance of a right-to-left shunt can be assessed more easily using transcranial Doppler ultrasound, with sensitivity and specificity similar to TEE.⁸

Based on the results of the extensive cardiology workups, patients were divided into 3 groups: AAA (n=40), PFO (n=153), and PAF (n=128) (Figure 1). AAA was considered as a cause of stroke if vulnerable AAA was observed on the TEE or MDCT. Vulnerable AAA was defined as aortic plaques in the ascending aorta or proximal arch that met ≥ 1 of the following criteria: (1) ≥ 4 mm of intima-media thickness on TEE or ≥ 6 mm of thickness adjacent to the aortic wall on MDCT or (2) ulcerated plaque or (3) mobile plaque on TEE or soft plaque on MDCT.^{9,10} We performed the TEE or transcranial Doppler ultrasound agitated saline test or MDCT to evaluate PFO. PFO was deemed present when 1 of following criteria was observed: (1) the passage of >3 microbubbles to the left atrium within 3 cardiac cycles after complete opacification of the right atrium on the TEE, (2) microembolic signals within 40 seconds after injection of agitated saline with microbubbles on the transcranial Doppler ultrasound, or (3) a distinct flap in the left atrium at the expected location of the septum primum or a continuous column of contrast material connecting both atria or jet of contrast material into the right atrium on the MDCT.^{11–13} Patients in the PAF group were those who had no history or ECG findings of atrial fibrillation at admission, but PAF was diagnosed using repetitive ECGs or 72-hour cardiac telemetry. If patients had PAF plus PFO or AAA, patients were classified as belonging to the PAF group because the current evidence-based classification system classifies PAF as a high-risk embolic source and PFO and AAA as low or uncertain sources of embolism.¹⁴ Few patients had both AAA and PFO, and they were excluded from this analysis.

Image Analysis

All participants underwent 3-T magnetic resonance imaging including DWI (Achieva; Phillips Medical System). In the

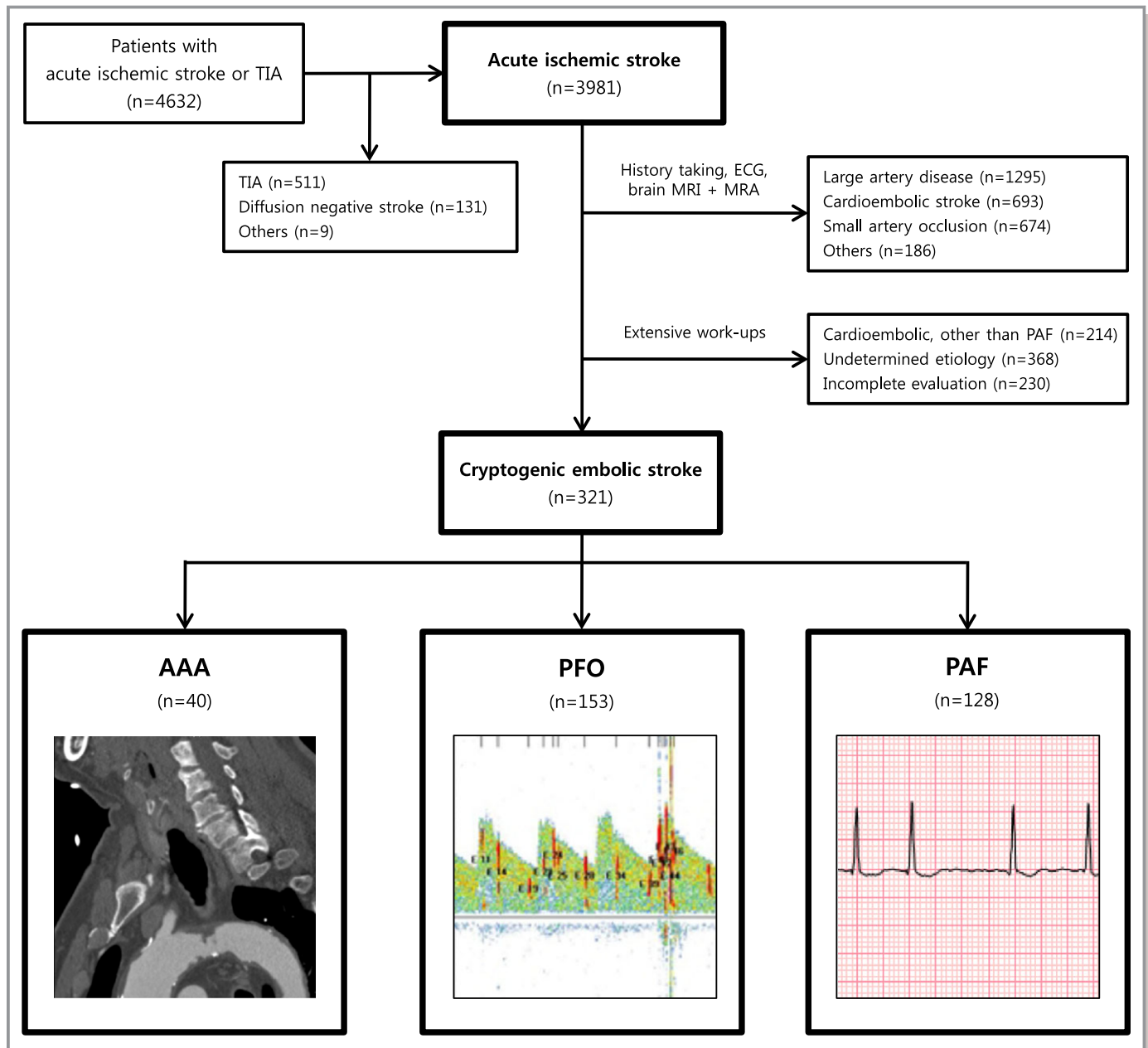


Figure 1. Patient selection. Among 368 patients excluded due to undetermined etiology, 21 had 2 of 3 embolic source categories. AAA indicates aortic arch atheroma; MRA, magnetic resonance angiography; MRI, magnetic resonance imaging; PAF, paroxysmal atrial fibrillation; PFO, patent foramen ovale; TIA, transient ischemic attack.

development set, the DWI parameters were as follows: repetition time 3000 ms, echo time 80 ms, matrix number 128×128, 2 b values of 0 and 1000 s/mm², slice thickness 5 mm, interslice gap 2 mm, 22 axial slices, and field of view 240 mm. In the validation set (Intera, Achieva; Philips Healthcare), the parameters were as follows: repetition time 3300, echo time 77 ms, matrix number 128×128, 2 b values of 0 and 1000 s/mm², slice thickness 5 mm, 28 axial slices, and field of view 220 mm. We analyzed lesions noted on DWI in terms of their size, number, and distribution. The largest

diameter of each lesion was measured, and each lesion was divided into small or large lesions based on a threshold of 20 mm. We manually counted the number of lesions on DWI. We evaluated DWI lesion distribution based on the involved structure (eg, cortex, subcortex, or both) or the involved vascular territory (eg, anterior or posterior circulation). The involvement of multiple vascular territories was noted when multiple lesions on DWI were located (1) in unilateral anterior and posterior circulation, (2) in bilateral anterior circulation, or (3) in bilateral anterior and posterior circulation.

Statistical Analysis

Descriptive demographic, clinical, and radiological data are shown as mean±SD or numbers and frequencies, as appropriate. We analyzed the differences among the groups using a chi-square or Mann–Whitney test for discrete variables and 1-way ANOVA or Kruskal–Wallis tests for continuous variables. We used a multinomial regression analysis to detect the clinical and DWI factors associated with the 3 groups: AAA, PFO, and PAF. To develop the prediction model, we used a generalized logit model for the nominal response data after selecting the variables with $P<0.05$ in the univariate analysis with the development data set. Multicollinearity was checked using a variance inflation factor; there were no variables with a variance inflation factor >10 . The Bonferroni method was

used to correct for multiple testing of three. The prediction model was validated externally in a different cohort ($n=117$). In all analyses, the area under the curve was calculated. All statistical analyses were performed using commercially available SPSS version 20 (IBM Corp), SAS version 9.3 (SAS Institute), and R version 3.1.1 (R Foundation for Statistical Computing). A 2-sided $P<0.05$ was considered statistically significant.

Results

Clinical Characteristics

Of the patients with embolic stroke of undetermined source at the time of admission, we included 321 patients with 1 of 3

Table 1. Clinical and Radiological Characteristics

	AAA (n=40)	PFO (n=153)	PAF (n=128)	P Value
Clinical characteristics				
Age, years, median (IQR)	72.5 (68.0–78.8)	56.0 (46.0–66.0)	72.0 (63.0–80.0)	<0.001
Male sex, n (%)	29 (72.5)	107 (69.9)	70 (54.7)	0.015
Hypertension, n (%)	33 (82.5)	57 (37.3)	88 (68.8)	<0.001
Diabetes mellitus, n (%)	6 (15.0)	24 (15.7)	23 (18.0)	0.844
Dyslipidemia, n (%)	16 (40.0)	34 (22.2)	35 (27.3)	0.087
Coronary artery disease, n (%)	2 (5.0)	6 (3.9)	12 (9.4)	0.162
Current smoker, n (%)	15 (37.5)	47 (30.7)	17 (13.3)	0.001
Metabolic syndrome, n (%)	4 (10.0)	19 (12.4)	15 (11.7)	0.971
Initial NIHSS, median (IQR)	1 (0–3)	1 (0–4)	7 (2–16)	<0.001
Radiological characteristics				
Size				
Largest diameter, mm, median (IQR)	11.8 (8.1–14.4)	16.4 (9.4–38.4)	47.9 (27.2–74.3)	<0.001
≥20 mm, n (%)	7 (17.5)	63 (41.2)	107 (83.6)	<0.001
Composition				
Small lesions only, n (%)	31 (77.5)	75 (49.0)	13 (10.2)	<0.001
Small and large lesions, mixed, n (%)	1 (2.5)	52 (34.0)	83 (64.8)	
Large lesions only, n (%)	8 (20.0)	26 (17.0)	32 (25.0)	
Distribution				
Involved vascular territory				
Posterior circulation, n (%)	5 (12.5)	65 (42.5)	21 (16.4)	<0.001
Multiple vascular territories, n (%)	19 (47.5)	17 (11.1)	9 (7.0)	<0.001
Involved structure				
Cortical lesions only, n (%)	9 (22.5)	33 (21.6)	39 (30.5)	0.211
Subcortical lesions only, n (%)	9 (22.5)	58 (37.9)	15 (11.7)	<0.001
Multiplicity				
Number of lesions, median (IQR)	4 (2–13)	1 (1–3)	1 (1–2)	<0.001
≥3 lesions, n (%)	29 (72.5)	49 (32.5)	30 (23.4)	<0.001

AAA indicates aortic arch atheroma; IQR, interquartile range; NIHSS, National Institutes of Health Stroke Scale; PAF, paroxysmal atrial fibrillation; PFO, patent foramen ovale.

etiologies: AAA in 40 (12.5%), PFO in 153 (47.7%), and PAF in 128 (39.9%) patients. Table 1 shows the clinical characteristics of these 3 groups. Patients with PFO were younger than patients in the other 2 groups (PFO: aged 55.5 years; AAA: aged 72.9 years; PAF: aged 71.6 years; $P<0.001$). Hypertension was more frequent in the AAA group ($P<0.001$). The proportion of current smokers was lowest among the PAF–stroke patients. PAF–stroke patients experienced the most severe neurological deficits at presentation (median NIHSS score: PAF 7 [interquartile range 2–16]; AAA 1 [interquartile range 0–3]; PFO 1 [interquartile range 0–4]; $P<0.001$).

Radiological Characteristics

The DWI lesion patterns were different among the 3 groups (Table 1 and Figure 2). Lesions in the AAA group were smaller than lesions in the other groups (largest lesion diameter: AAA: 11.8 mm; PFO: 16.4 mm; PAF: 47.9 mm; $P<0.001$). Most of the patients (77.5%) in the AAA group had only small lesions, whereas patients in the PAF group showed larger lesions; many of them (64.8%) had no small lesions. Involved vascular territories and anatomical structures were also different. Approximately half of the patients (47.5%) with AAA showed lesions in multiple vascular territories, whereas involvement of a single vascular territory was more frequent in the PFO and PAF groups (88.9% and 93.0%, respectively; $P<0.001$). A higher proportion of patients in the PFO group had lesions

involving posterior circulation compared with other groups (PFO: 42.5%; AAA: 12.5%; PAF: 16.4%; $P<0.001$). More than one-third of PFO patients (37.9%) had lesions restricted to the subcortical areas ($P<0.001$). In terms of lesion multiplicity, the AAA group had a greater number of lesions compared with the PFO and PAF groups (median DWI lesion number: AAA: 4; PFO: 1; PAF: 1; $P<0.001$). Thirty-two patients (80.0%) in the AAA group showed multiple lesions on DWI, whereas more than half of the patients in the other groups had a single lesion (PFO: 55.6%; PAF: 60.9%).

The Prediction Model for AAA, PFO, and PAF

The prediction model was constructed using the development data set ($n=321$). We selected the following aforementioned variables: age, hypertension, current cigarette smoking, initial NIHSS score, the presence of large lesions (largest lesion diameter ≥ 20 mm), subcortical involvement, posterior circulation involvement, multiple vascular territory involvement, and lesion multiplicity (≥ 3 lesions) (Table 2). NIHSS scores were transformed using a natural log considering its skewed distribution. Age, hypertension, initial NIHSS score, large lesion presence, posterior circulation involvement, multiple vascular territory involvement, and lesion multiplicity were independent predictors of AAA, PFO, and PAF (pseudo, $R^2=0.656$). Based on these results, the probability equations for each group were generated:

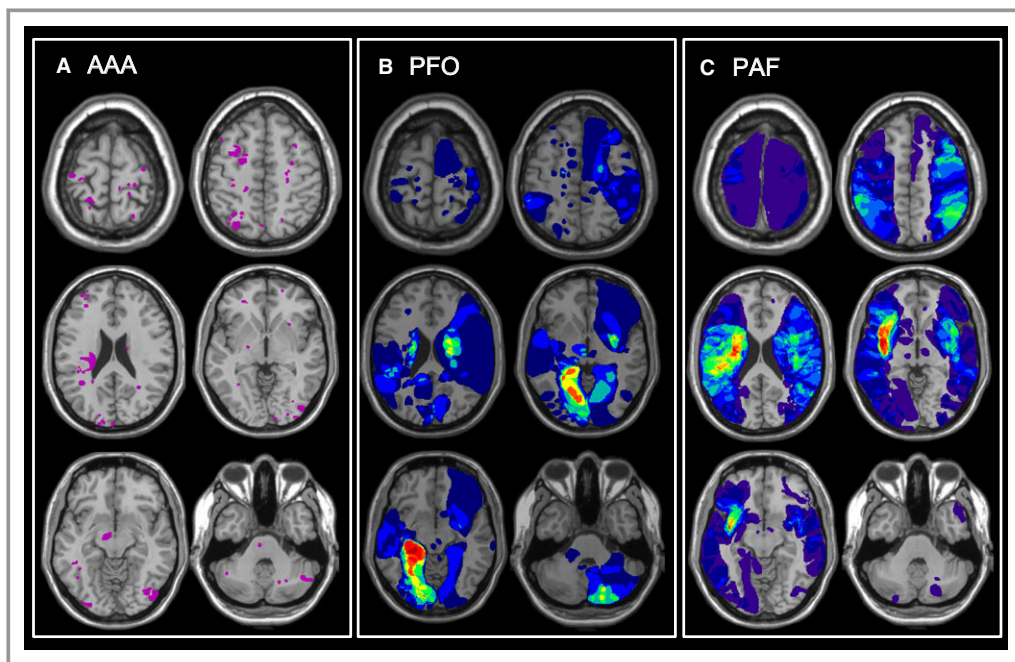


Figure 2. Contour images of the mean values of the affected areas among the 3 groups: (A) AAA group, (B) PFO group, and (C) PAF group. AAA indicates aortic arch atheroma; PAF, paroxysmal atrial fibrillation; PFO, patent foramen ovale.

Table 2. Multinomial Logistic Regression Analysis for AAA, PFO, and PAF

				PFO vs AAA*		PAF vs PFO*		PAF vs AAA*	
	Chi-Square	df	Overall P Value	OR (95% CI)	P Value	OR (95% CI)	P Value	OR (95% CI)	P Value
Age	40.9	2	<0.001	0.88 (0.82–0.93)	<0.001	1.08 (1.04–1.12)	0.001	0.95 (0.89–1.01)	0.164
NIHSS	8.3	2	0.016	1.43 (0.7–2.93)	0.694	1.53 (0.95–2.47)	0.098	2.19 (1.06–4.55)	0.030
Hypertension	8.7	2	0.013	0.26 (0.07–1.04)	0.059	2.24 (0.96–5.23)	0.068	0.59 (0.14–2.51)	1.000
Current smoking	5.0	2	0.081	0.4 (0.11–1.45)	0.261	0.65 (0.24–1.76)	0.915	0.26 (0.06–1.1)	0.075
Large lesion (≥20 mm)	20.8	2	<0.001	3.21 (0.72–14.42)	0.189	4.12 (1.56–10.88)	0.002	13.24 (2.82–62.2)	<0.001
Involving posterior circulation	7.4	2	0.025	3.86 (0.72–20.79)	0.166	0.4 (0.15–1.06)	1.000	1.56 (0.26–9.17)	0.072
Involving subcortex	2.6	2	0.266	0.69 (0.14–3.32)	1.000	0.55 (0.19–1.58)	0.528	0.38 (0.07–2.03)	0.503
Multiple vascular territories	9.4	2	0.009	0.23 (0.05–1.02)	0.054	0.53 (0.11–2.49)	0.983	0.12 (0.02–0.69)	0.011
Multiple lesions (≥3 lesions)	11.7	2	0.003	0.44 (0.11–1.87)	0.530	0.33 (0.12–0.9)	0.025	0.15 (0.03–0.67)	0.007

AAA indicates aortic arch atheroma; NIHSS, National Institutes of Health Stroke Scale; OR, odds ratio; PAF, paroxysmal atrial fibrillation; PFO, patent foramen ovale.
 *Indicates reference group used in the analyses.

$$\text{Probability (AAA)} = \frac{1}{1 + [\text{Probability (PFO)} + \text{Probability (PAF)}]}$$

$$\text{Probability (PFO)} = \frac{\exp[\text{Prediction score (PFO)}]}{(1 + \exp[\text{Prediction score (PFO)}] + \exp[\text{Prediction score (PAF)}])}$$

$$\text{Probability (PAF)} = \frac{\exp[\text{Prediction score (PAF)}]}{(1 + \exp[\text{Prediction score (PFO)}] + \exp[\text{Prediction score (PAF)}])}$$

The following equations for the PFO and PAF prediction scores were generated using the results from a generalized logit model (Table 3): prediction score (PFO)=10.200–0.124×age (yr)+0.366×ln (NIHSS score+1)–1.357×hypertension+1.321×large lesion+1.090×posterior lesion–0.905×multiple lesion–1.255×multiple territory; Prediction score (PAF)=3.104–0.038×age (yr)+0.799×ln (NIHSS score+1)–0.567×hypertension+2.883×large lesion+0.112×posterior lesion–1.951×multiple lesion–1.794×multiple territory (for categorical variables, “1” was entered if the variable was indicated; otherwise, “0” was entered) (Data S1). The area under the curve of the prediction model was 0.79 (95% CI 0.76–0.82) based on the development data set, which we used for internal validation.

Table 3. Multivariable Associations of the Selected Factors With AAA, PFO, and PAF

	AAA* vs PFO		AAA* vs PAF		PFO* vs PAF	
	P Value	Coefficient	P Value	Coefficient	P Value	Coefficient
Intercept		10.200		3.104		–7.096
Age	<0.001	–0.124	0.438	–0.038	<0.001	0.086
NIHSS [†]	0.655	0.366	0.024	0.799	0.087	0.433
Hypertension	0.396	–1.357	0.982	–0.567	0.070	0.790
Large lesion (≥20 mm)	0.095	1.321	<0.001	2.883	<0.001	1.561
Involving posterior circulation	0.252	1.090	>0.999	0.112	0.041	–0.979
Multiple vascular territories	0.101	–1.255	0.031	–1.794	>0.999	–0.540
Multiple lesions (≥3 lesions)	0.101	–0.905	0.002	–1.951	0.030	–1.046

AAA indicates aortic arch atheroma; NIHSS, National Institutes of Health Stroke Scale; PAF, paroxysmal atrial fibrillation; PFO, patent foramen ovale.
 *Indicates reference group used in the analyses.
[†]NIHSS was transformed using natural log, ln (NIHSS+1).

External Validation of the Prediction Model

The clinical and radiological characteristics from the validation data set (n=117) were comparable with the development data set (Table 4). The prediction ability of the model was adequate in the validation cohort, with an area under the curve of 0.78 (95% CI 0.68–0.86). When a patient was allocated to the highest predicted probability among the 3 groups, the accuracy was 72.7%. Three representative cases with application of prediction models for AAA, PFO, and PAF are shown in Figure 3.

Discussion

In the present study, we observed distinct clinical and radiological characteristics for AAA, PFO, and PAF patients. Based on these characteristics, we developed an equation to predict the most probable etiology underlying cryptogenic embolisms.

Our data showed that the clinical features and lesion topography (infarct pattern and distribution) might provide clues regarding the causes of embolic stroke of undeter-

mined source. This knowledge of the clinical and radiological features of embolic strokes of undetermined source will help physicians understand the pathogenic mechanisms involved in stroke development.³ Interestingly, vascular risk factor profile and infarct pattern were quite distinct among the 3 causes of embolic stroke of undetermined source. PFO primarily consisted of younger patients with a relatively healthy risk factor profile and posterior distribution, whereas AAA consisted of elderly patients with a high-risk profile and small cortical or border zone infarcts. PAF consisted of elderly patients with a relatively healthy risk factor profile (compared with those with AAA) and large cortical infarcts.

Our results are in line with previous PFO studies investigating the clinical characteristics and DWI patterns of PFO-related stroke from component databases in the RoPE study⁷ and the autopsy study of cholesterol emboli from vulnerable AAA.¹⁵ A brain single-photon emission computed tomography study showed that during the Valsalva maneuver, the rate of blood flow in the posterior circulation was higher than that in the anterior circulation, which could be a possible explanation

Table 4. Comparison of Clinical and Radiological Characteristics Between the Development Data Set and the Validation Data Set

	Samsung Medical Center (n=321)	Ajou University Hospital (n=117)	P Value
Clinical characteristic			
Age, years, median (IQR)	66.0 (54.5–75.0)	62.0 (50.0–73.0)	0.081
Male sex, n (%)	206 (64.2)	73 (62.4)	0.732
Hypertension, n (%)	178 (55.5)	71 (60.7)	0.328
Diabetes mellitus, n (%)	53 (16.5)	15 (12.8)	0.345
Dyslipidemia, n (%)	85 (26.5)	27 (23.1)	0.470
Coronary artery disease, n (%)	20 (6.2)	10 (8.5)	0.396
Current smoker, n (%)	79 (24.6)	25 (21.4)	0.480
Metabolic syndrome, n (%)	101 (31.9)	47 (40.2)	0.105
Initial NIHSS, median (IQR)	3 (1–8)	3 (1–7)	0.661
Radiological characteristics			
Size			
Largest diameter, ≥20 mm, n (%)	117 (55.1)	75 (64.1)	0.093
Distribution			
Involved vascular territory			
Posterior circulation, n (%)	91 (28.3)	29 (24.8)	0.459
Multiple vascular territories, n (%)	45 (14.0)	14 (12.0)	0.578
Involved structure			
Cortical lesions only, n (%)	81 (25.2)	38 (32.8)	0.119
Subcortical lesions only, n (%)	82 (25.5)	25 (21.4)	0.368
Multiplicity			
Number of lesions, ≥3 lesions, n (%)	108 (33.9)	33 (28.2)	0.264

IQR indicates interquartile range; NIHSS, National Institutes of Health stroke scale.

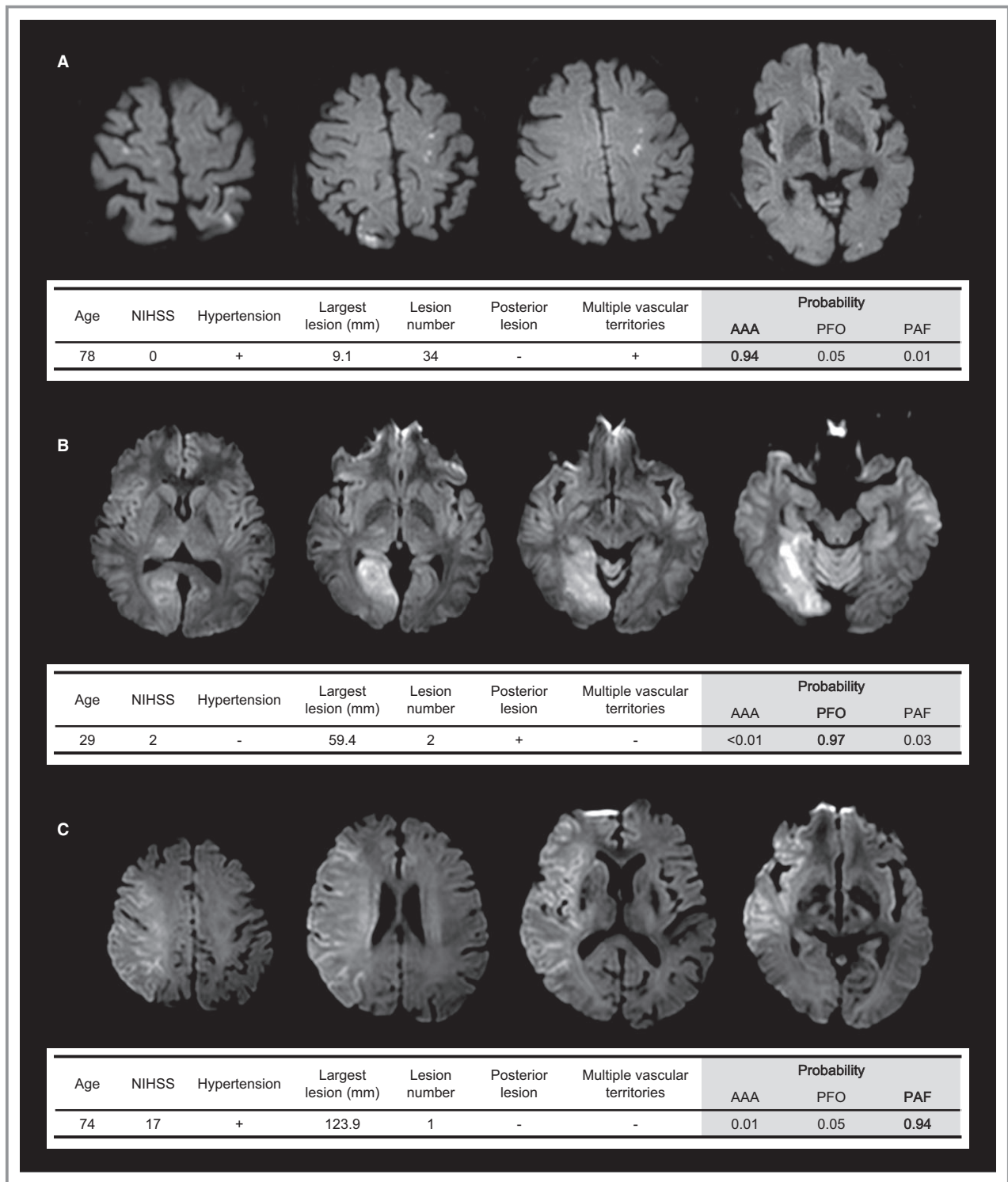


Figure 3. Examples applying the prediction model to real clinical practice. A, A male patient aged 78 years had multiple small infarcts in multiple vascular territories. According to the prediction model, the probabilities for AAA, PFO, and PAF were 0.94, 0.05, and 0.01, respectively. We performed ECG, 72-hour Holter monitoring, and a transcranial Doppler shunt test; the results were negative. Multidetector row computed tomography revealed thick atheroma in the ascending aorta. B, A female patient aged 29 years had a right PCA infarction. There was no lesion outside the right PCA territory. The probability of PFO was 0.97. On transesophageal echocardiography, PFO with right-to-left shunt was observed. C, This is a case of a territorial right middle cerebral artery infarction. The patient was aged 74 years; initial NIHSS was 17. The PAF probability was 0.94. Although we did not find an abnormality on serial ECGs, 72-hour cardiac telemonitoring showed paroxysmal atrial fibrillation. AAA indicates aortic arch atheroma; NIHSS, National Institutes of Health Stroke Scale; PAF, paroxysmal atrial fibrillation; PCA, posterior cerebral artery; PFO, patent foramen ovale.

for the posterior predominance of paradoxical embolism.¹⁶ In contrast, because the clots from the left atrium or left atrial appendix are usually large (fibrin-containing), atrial fibrillation is associated with more severe ischemic strokes and longer (>60 minutes) transient ischemic attacks compared with arteroembolic strokes from the carotid artery or aortic arch (cholesterol-containing). Clot components reportedly determine infarct patterns; an autopsy study revealed that emboli containing fibrin often cause large cortical infarcts, whereas emboli containing cholesterol crystals frequently result in small border zone infarcts.¹⁷

When investigating the underlying causes of embolic stroke of undetermined source, physicians need to decide on the type and extent of the ancillary procedures they will use to document a precise embolic source for proper secondary preventive management. In clinical practice, routinely ordering diagnostic tests, including TEE, and workups for paradoxical embolism and deep vein thrombosis, aortogenic embolism, and prolonged cardiac telemonitoring is neither indicated nor possible. TEE is considered the gold standard for the evaluation of embolic stroke of undetermined source; however, routine application of TEE is often limited in patients with acute stroke because of acute illness, mental change, coagulopathy or bleeding tendency, and lack of patient cooperation. The use of more noninvasive diagnostic techniques, such as the MDCT to detect aortogenic embolism^{18,19} or transcranial right-to-left shunt test to detect paradoxical embolism,⁸ would be practical alternatives. In contrast, current guidelines recommend performing cardiac monitoring for at least 24 hours to detect PAF²⁰; however, an atrial fibrillation detection rate of 24-hour Holter monitoring does not seem to be sufficient, so long-term cardiac rhythm monitoring should be considered in patients with a high probability of having PAF.

Moreover, the yield of diagnostic tests may differ among patients, depending on the probability of having PFO, AAA, and PAF as a cause of stroke. The yield (positive predictive value and probability of stroke cause) of cardiac telemonitoring, for example, and the workup for paradoxical embolism and deep vein thrombosis are very different. Based on a report by the US Centers for Medicare and Medicaid Services, aggregate cost for intensive embolic source evaluation in a single ischemic stroke patient can be >\$2000 (ie, ECG, \$17; complete transthoracic echocardiography, \$229; transcranial Doppler ultrasound, \$290; diagnostic TEE, \$308; MDCT, \$420; and cardiac telemetry, \$680). Considering the increasing number of stroke patients, inadvertent etiologic evaluations could be a great burden to the economy. Consequently, selecting appropriate cardiologic workups for individual patients based on the probability equation would improve the cost-effectiveness of advanced diagnostic technologies and may help with timely etiologic investigation and accurate diagnosis.

Limitations

The current study has the advantage of incorporating derivation and external validation data, but it also has several limitations. Most important, not all patients in this study underwent the same diagnostic workups. Although all patients underwent DWI and magnetic resonance angiography, the cardiac workups, which included TEE, MDCT, and cardiac telemonitoring, varied among patients, depending on the physician's preference in real-world practice. Patients who were likely to have aortogenic or paradoxical embolism, for example, received additional TEE more often, whereas those who were suspected of having PAF received cardiac telemonitoring more often. Nevertheless, the external validation analysis using data from a different medical center suggested that the physician's preference did not significantly influence our conclusions. In addition, we hypothesized that it is important to differentiate embolism cause in patients with embolic stroke of undetermined source because different treatment strategies are required (eg, plaque stabilizer [ie, statin] for AAA, closure [in some cases] for PFO, and anticoagulation for PAF); however, this is beyond the scope of the current analysis. Further studies with prospective follow-up data are needed to test this hypothesis. Last, these data are from 2 centers in South Korea; therefore, the generalizability of our results may be limited. Future studies with a prospective design including different ethnic populations are warranted.

Conclusions

Our data indicate that patients with embolic stroke of undetermined source showed distinct clinical and radiological features depending on the underlying stroke cause. Specific diagnostic tests for aortocardiac sources could be guided by such features. Our probability equations can aid decision making by identifying patients who are likely to have PAF during hospitalization in the first days of stroke onset or, conversely, those likely to have aortogenic pathology or paradoxical embolic sources. Continuous efforts are needed to refine the approach to working up cases of suspected embolic stroke of undetermined source, incorporating other biomarkers, such as B-type natriuretic peptide²¹ or genetic risk factors.²²

Acknowledgments

We thank Seonwoo Kim, PhD, Division of Biostatistics, Samsung Biomedical Research Institute, who assisted with data analysis without any compensation the contribution.

Sources of Funding

This study was supported by the Korean Health Technology R&D Project, Ministry of Health and Welfare, Republic of

Korea (HI14C16240000). The funder had no influence on design and conduct of the study; collection, management, analysis, and interpretation of the data; and preparation, review, or approval of the manuscript.

Disclosures

None.

References

- Sacco RL, Ellenberg JH, Mohr JP, Tatemichi TK, Hier DB, Price TR, Wolf PA. Infarcts of undetermined cause: the NINCDS Stroke Data Bank. *Ann Neurol*. 1989;25:382–390.
- Amarenco P. Cryptogenic stroke, aortic arch atheroma, patent foramen ovale, and the risk of stroke. *Cerebrovasc Dis*. 2005;20:68–74.
- Bang OY, Ovbiagele B, Kim JS. Evaluation of cryptogenic stroke with advanced diagnostic techniques. *Stroke*. 2014;45:1186–1194.
- Fisher ES, Bynum JP, Skinner JS. Slowing the growth of health care costs—lessons from regional variation. *N Engl J Med*. 2009;360:849–852.
- Harloff A, Handke M, Reinhard M, Geibel A, Hetzel A. Therapeutic strategies after examination by transesophageal echocardiography in 503 patients with ischemic stroke. *Stroke*. 2006;37:859–864.
- Kent DM, Thaler DE. Is patent foramen ovale a modifiable risk factor for stroke recurrence? *Stroke*. 2010;41:S26–S30.
- Kent DM, Ruthazer R, Weimar C, Mas JL, Serena J, Homma S, Di Angelantonio E, Di Tullio MR, Lutz JS, Elkind MS, Griffith J, Jaigobin C, Mattle HP, Michel P, Mono ML, Nedeltchev K, Papetti F, Thaler DE. An index to identify stroke-related vs incidental patent foramen ovale in cryptogenic stroke. *Neurology*. 2013;81:619–625.
- Droste DW, Schmidt-Rimpler C, Wichter T, Dittrich R, Ritter M, Stypmann J, Ringelstein EB. Right-to-left-shunts detected by transesophageal echocardiography and transcranial Doppler sonography. *Cerebrovasc Dis*. 2004;17:191–196.
- Amarenco P, Cohen A, Tzourio C, Bertrand B, Hommel M, Besson G, Chauvel C, Touboul PJ, Boussier MG. Atherosclerotic disease of the aortic arch and the risk of ischemic stroke. *N Engl J Med*. 1994;331:1474–1479.
- Kim SJ, Ryoo S, Hwang J, Noh HJ, Park JH, Choe YH, Bang OY. Characterization of the infarct pattern caused by vulnerable aortic arch atheroma: DWI and multidetector row CT study. *Cerebrovasc Dis*. 2012;33:549–557.
- Lee JY, Song JK, Song JM, Kang DH, Yun SC, Kang DW, Kwon SU, Kim JS. Association between anatomic features of atrial septal abnormalities obtained by omni-plane transesophageal echocardiography and stroke recurrence in cryptogenic stroke patients with patent foramen ovale. *Am J Cardiol*. 2010;106:129–134.
- Kim JW, Kim SJ, Yoon CW, Park CH, Kang KW, Kim SK, Kim YH, Bang OY. Association between the amount of right-to-left shunt and infarct patterns in patients with cryptogenic embolic stroke: a transcranial Doppler study. *Int J Stroke*. 2013;8:657–662.
- Williamson EE, Kirsch J, Araoz PA, Edmister WB, Borgeson DD, Glockner JF, Breen JF. ECG-gated cardiac CT angiography using 64-MDCT for detection of patent foramen ovale. *AJR Am J Roentgenol*. 2008;190:929–933.
- Ay H, Furie KL, Singhal A, Smith WS, Sorensen AG, Koroshetz WJ. An evidence-based causative classification system for acute ischemic stroke. *Ann Neurol*. 2005;58:688–697.
- Ezzeddine MA, Primavera JM, Rosand J, Hedley-Whyte ET, Rordorf G. Clinical characteristics of pathologically proved cholesterol emboli to the brain. *Neurology*. 2000;54:1681–1683.
- Hayashida K, Fukuchi K, Inubushi M, Fukushima K, Imakita S, Kimura K. Embolic distribution through patent foramen ovale demonstrated by (99 m)Tc-MAA brain SPECT after valsalva radionuclide venography. *J Nucl Med*. 2001;42:859–863.
- Masuda J, Yutani C, Ogata J, Kuriyama Y, Yamaguchi T. Atheromatous embolism in the brain: a clinicopathologic analysis of 15 autopsy cases. *Neurology*. 1994;44:1231–1237.
- Kim SJ, Choe YH, Park SJ, Kim GM, Chung CS, Lee KH, Bang OY. Routine cardiac evaluation in patients with ischaemic stroke and absence of known atrial fibrillation or coronary heart disease: transthoracic echocardiography vs. multidetector cardiac computed tomography. *Eur J Neurol*. 2012;19:317–323.
- Hussain SI, Gilkeson RC, Suarez JJ, Tarr R, Schluchter M, Landis DM, Zaidat OO. Comparing multislice electrocardiogram-gated spiral computerized tomography and transesophageal echocardiography in evaluating aortic atheroma in patients with acute ischemic stroke. *J Stroke Cerebrovasc Dis*. 2008;17:134–140.
- Jauch EC, Saver JL, Adams HP Jr, Bruno A, Connors JJ, Demaerschalk BM, Khatri P, McMullan PW Jr, Qureshi AI, Rosenfield K, Scott PA, Summers DR, Wang DZ, Wintermark M, Yonas H. Guidelines for the early management of patients with acute ischemic stroke: a guideline for healthcare professionals from the American Heart Association/American Stroke Association. *Stroke*. 2013;44:870–947.
- Rodriguez-Yanez M, Arias-Rivas S, Santamaria-Cadavid M, Sobrino T, Castillo J, Blanco M. High pro-BNP levels predict the occurrence of atrial fibrillation after cryptogenic stroke. *Neurology*. 2013;81:444–447.
- Jickling GC, Stamova B, Ander BP, Zhan X, Liu D, Sison SM, Verro P, Sharp FR. Prediction of cardioembolic, arterial, and lacunar causes of cryptogenic stroke by gene expression and infarct location. *Stroke*. 2012;43:2036–2041.